APPENDIX

Table II[15–18] gives the results of paramagnetic-resonance measurements on all trivalent rare-earth ions in tetragonal sites in $CaWO_4$.

TABLE II. g values and eigenvectors for trivalent rare-earth ions in tetragonal sites in calcium tungstate.

Ion	Ground manifold	Observed $g_{\parallel}$	Lowest level (derived from observed $g_{\parallel}$ assuming no mixing from higher manifolds)	Calculated $g_{\perp}$	Observed $g_{\perp}$	Irreducible rep^{r} in S_4	Reference
Ce^{3+}	$^2F_{5/2}$	2.915	$0.895\|\pm\frac{5}{2}\rangle+0.447\|\mp\frac{3}{2}\rangle$	1.534	1.423	$(^1\Gamma_5,^1\Gamma_6)$	5
Pr^{3+}	$^3H_4$	...	No ESR observed at 9 and 36 Gc/sec	...	...		This paper
Nd^{3+}	$^4I_{9/2}$	2.035	$0.6828\|\pm\frac{9}{2}\rangle+0.5407\|\pm\frac{1}{2}\rangle+0.4916\|\mp\frac{7}{2}\rangle$	[a]	2.533	$(^1\Gamma_7,^1\Gamma_8)$	15, 16
Pm^{3+}	$^5I_4$	...	...	...	...	...	...
Sm^{3+}	$^6H_{5/2}$	0.4396	$0.753\|\pm\frac{5}{2}\rangle+0.658\|\mp\frac{3}{2}\rangle$[b]	0.633	0.6416	$(^1\Gamma_5,^1\Gamma_6)$	17
Eu^{3+}	$^7F_0$	...	...	...	...	...	...
Gd^{3+}	$^8S_{7/2}$	1.9915	...	...	1.9916	...	3
Tb^{3+}	$^7F_6$	17.777	$a\|6\rangle+b\|2\rangle+c\|-2\rangle+d\|-6\rangle$	0	<0.15	$^1\Gamma_2$	7
Dy^{3+}	$^6H_{15/2}$	7.267	Data insufficient to obtain eigenvector	...	5.466	...	18
Ho^{3+}	$^5I_8$	13.691	$\alpha\|\pm7\rangle+\beta\|\pm3\rangle+\gamma\|\mp1\rangle+\delta\|\mp5\rangle$[c]	0	$\simeq0$	$(^1\Gamma_3,^1\Gamma_4)$	This paper
Er^{3+}	$^4I_{15/2}$	1.251	$\|\pm\frac{1}{2}\rangle$[d]	9.6	8.401	$(^1\Gamma_5,^1\Gamma_6)$	18
Tm^{3+}	$^3H_6$	...	No ESR at 9 and 36 Gc/sec	...	...	...	This paper
Yb^{3+}	$^2F_{7/2}$	1.055	$0.702\|\pm\frac{5}{2}\rangle+0.714\|\mp\frac{3}{2}\rangle$	3.969	3.914	$(^1\Gamma_5,^1\Gamma_6)$	5

[a] Both g values were needed to obtain the eigenvector so that there is no check on its correctness. However, $Ag_{\perp}/Bg_{\parallel}=0.97$ rules out mixing from $^4I_{11/2}$.
[b] The agreement between experimental and predicted values of $g_{\perp}$ is fortuitous. $Ag_{\perp}/Bg_{\parallel}=0.38$ indicates important mixing from $^6H_{7/2}$.
[c] In the absence of Jahn-Teller splitting.
[d] Predicted $g_{\parallel}$ for pure $|\pm\frac{1}{2}\rangle$ state is 1.200.

[15] U. Ranon, Phys. Letters **8**, 154 (1964).
[16] N. E. Kask, L. S. Kornienko, A. M. Prokhorov, and M. Fakir, Fiz. Tverd. Tela **5**, 2303 (1963) [English transl.: Soviet Phys.—Solid State **5**, 1675 (1964)].
[17] J. Kirton, Phys. Letters **16**, 209 (1965).
[18] J. Kirton (unpublished).

PHYSICAL REVIEW VOLUME 139, NUMBER 6A 13 SEPTEMBER 1965

Rare-Earth Ion Relaxation Time and G Tensor in Rare-Earth-Doped Yttrium Iron Garnet. I. Ytterbium

BARRY H. CLARKE,* K. TWEEDALE, AND R. W. TEALE†
Mullard Research Laboratories, Redhill, Surrey, England
(Received 26 April 1965)

Microwave-resonance measurements at 9.3 and 16.8 Gc/sec between 1.5 and 300°K in the principal crystallographic directions of a single-crystal of yttrium iron garnet (YIG) doped with 5.1% Yb are compared with the predictions of the longitudinal (so-called "slow relaxing ion") mechanism of relaxation, which is briefly reviewed. Except for the low-temperature anomaly in the [110] direction, excellent agreement is found. A quantitative analysis allows deduction of the tensor G describing the anisotropic exchange splitting of the ground-state Kramers doublet of the Yb ion. We obtain $G_1=31.9$ cm^{-1}; $G_2=22.4$ cm^{-1}; $G_3=8.5$ cm^{-1}, which is a similar result to that reported from spectroscopic measurements on ytterbium iron garnet. The small differences probably reflect the different lattice dimensions in the two cases. We also deduce τ, the relaxation time of the Yb ion in the YIG environment. The results are most extensive and accurate in the [111] direction, where the temperature dependence for $T<60$°K indicates the dominance of a direct process as described by $(1/\tau)_D=(1/\tau^0)_D\coth(\delta/2kT)$ with $(1/\tau^0)_D=2.1\times10^9$ sec^{-1} for $\delta_{111}=21.0$ cm^{-1}. Taking into account that the measured relaxation time in this direction is a weighted average of the two relaxation times associated with the two values of the doublet splitting, we find that the observed direct process is well described by spin-magnon relaxation, which also gives a more consistent evaluation of the G tensor than does spin-lattice relaxation. At higher temperatures, the temperature dependence of the observed relaxation time follows that expected for the Raman process, viz., $(1/\tau)_R=AJ_8T^9$, with $A=4.5\times10^{-12}$ sec^{-1} (°K)$^{-9}$ for a Debye temperature of 550°K. This is in excellent agreement with the Raman-process relaxation time reported for Yb in yttrium gallium garnet, though it is some 5 orders of magnitude shorter than the theoretical estimate. The Orbach process is found to be unimportant over the temperature range covered.

1. INTRODUCTION

THE presence of small amounts of rare-earth (RE) ions profoundly modifies the ferrimagnetic resonance properties of YIG (yttrium iron garnet). Thus the resonance linewidth ΔH is considerably broadened, and depends in a complicated way on temperature, microwave frequency, and crystallographic direction. Furthermore, the value of the applied field for resonance

* Now at I.C.I. Fibres Ltd., Harrogate, Yorkshire, England.
† Now at The University, Sheffield, Yorkshire, England.

is shifted from that expected on the basis of the anisotropy measured by a static method, and this dynamic shift S_D is also a complex function of temperature, frequency, and direction.

The relaxation mechanism underlying this behavior has long been of interest. For Yb in YIG,[1] and to some extent for europium iron garnet[2] and for Er in YIG,[3] the main features of the experimental results can be understood in terms of a longitudinal (so-called "slow relaxing ion") mechanism. The purpose of this paper is to make a detailed interpretation of resonance measurements for 5.1% Yb in YIG in terms of the longitudinal mechanism. We will deduce the tensor G, describing the anisotropic splitting of the ground-state Kramers doublet of the Yb^{3+} ion. We will also derive the relaxation time of the Yb^{3+} ion, and compare this with current theories.

2. RELAXATION BY RE IONS

To aid the description of how the longitudinal mechanism operates in RE-doped YIG, we will briefly recall the magnetic structure.[4] In the molecular-field approximation, the Fe^{3+} ions form two sublattices which are strongly coupled together by an exchange field of the order of 6×10^6 Oe. This is the strongest interaction in the system, and the two sublattices can be considered, therefore, as a single resultant sublattice. The RE ions are coupled to this ferric sublattice with an exchange field which is roughly an order of magnitude less than the ferric-ferric exchange field. The RE-RE exchange interaction is at least another order of magnitude smaller, even for a high level of RE doping, and can be ignored for the small dopings with which we are concerned here. Thus the total system can be considered to a good approximation as a collection of isolated RE ions individually coupled to the resultant ferric sublattice.

The Fe^{3+} ions, being S-state, are weakly coupled to the phonon and magnon spectra, as evidenced by the narrow linewidth of well-polished, pure YIG. The RE ions, however, have nonzero orbital angular momentum and a large spin-orbit interaction. They are therefore coupled strongly to the lattice, either directly through phonon modulation of the crystal field or exchange field, or indirectly via magnon modulation of the exchange field. The relaxation time τ of the RE ions is therefore short compared to that of the ferric sublattice alone. But the RE ions indirectly couple the Fe^{3+} ions to the lattice, so that in a resonance experiment exciting the uniform or $k=0$ mode, the RE ions act as a leak to the lattice for the precessional energy of this mode, which is thereby damped, or, in other words, the resonance line is broadened.

Having outlined the physical basis whereby the RE ions relax the uniform mode, we will now discuss the mechanism by which this is effected. Two possible mechanisms have been proposed, a transverse and a longitudinal. These are named from the time-varying exchange field components which are effective in the relaxation. The two mechanisms are not contradictory, and under appropriate conditions, both may contribute significantly to the observed linewidth. The experimental evidence[1–3] suggests, however, that it is the longitudinal mechanism which is responsible for the observed linewidth and dynamic shift in the field for resonance below room temperature. Though we shall briefly consider the transverse mechanism in evaluating the relaxation times in the room-temperature region, we shall not describe the mechanism here, and the reader is referred to the literature[5] for details.

3. THE LONGITUDINAL MECHANISM

The longitudinal mechanism has long been known in the field of paramagnetic relaxation.[6] Its applicability to the case of RE ions in YIG was first proposed at the Kyoto Magnetism Conference by Van Vleck[7] from a suggestion by Obata, and by Dillon.[8] Teale and Tweedale[1] obtained the longitudinal mechanism formulas for linewidth and shift in the field for resonance by adapting the formulas of a formally similar model introduced by Clogston[9] to explain relaxation losses involving migratory electrons in ferrites. Van Vleck and Orbach,[10] and independently Madame Hartmann-Boutron,[11] obtained the formulas by solving the equation of motion of the uniform precession mode coupled to the RE ions. M. Hartmann-Boutron has also demonstrated the equivalence of this latter method to the "free-energy" method implicit in Teale and Tweedale's adaptation.

Here we will review the longitudinal mechanism as applied to RE ions in YIG, referring the reader to the literature[9–12] for detailed derivations of the formulas.

In the resonance experiment at frequency ω, the ferric sublattice precesses at this frequency about the direction of an applied static magnetic field. Conse-

[1] R. W. Teale and K. Tweedale, Phys. Letters **1**, 298 (1962).
[2] R. C. LeCraw, W. G. Nilsen, J. P. Remeika, and J. H. van Vleck, Phys. Rev. Letters **11**, 490 (1963).
[3] B. H. Clarke, R. F. Pearson, R. W. Teale, and K. Tweedale, J. Appl. Phys. **34**, 1269 (1963).
[4] R. Pauthenet, Ann. Phys. **3**, 424 (1958).
[5] C. Kittel, Phys. Rev. **115**, 1587 (1959); P. G. De Gennes, C. Kittel, and A. M. Portis, *ibid.* **116**, 323 (1959); C. Kittel, J. Appl. Phys. **31**, 11S (1960).
[6] See for instance, C. J. Gorter, *Paramagnetic Relaxation* (Elsevier Publishing Company, Amsterdam, 1947).
[7] J. H. van Vleck, J. Phys. Soc. Japan **17**, Suppl. B-I, 352 (1962).
[8] J. F. Dillon, Jr., J. Phys. Soc. Japan **17**, Suppl. B-I, 376 (1962). See also J. F. Dillon, Jr., Phys. Rev. **127**, 1495 (1962).
[9] A. M. Clogston, Bell System Tech. J. **34**, 739 (1955).
[10] J. H. van Vleck and R. Orbach, Phys. Rev. Letters **11**, 65 (1963).
[11] F. Hartmann-Boutron, Compt. Rend. **256**, 4412 (1963); J. Appl. Phys. **35**, 889 (1964); Phys. Condensed Matter **2**, 80 (1964).
[12] J. H. van Vleck, J. Appl. Phys. **35**, 882 (1964).

quently, the exchange field acting on the RE ions also precesses at this frequency. In the longitudinal mechanism, it is the time-varying component of the exchange field parallel to the direction of the RE spin which effects the relaxation. This component modulates the Zeeman splitting of the RE ions at the frequency ω. At a nonzero temperature, therefore, a redistribution of populations is required during a precession cycle to maintain the Boltzmann distribution between the Zeeman levels. As the RE ions relax not instantaneously, but in a finite time τ, the populations lag behind the values appropriate to the instantaneous magnitude of the longitudinal component of the exchange field. Energy is therefore passed from the precession of the ferric sublattice to the RE ions, and thence to the lattice as indicated previously.

Now in the usual low power resonance experiment, the angle of precession is very small, so that the component of the exchange field in the average direction of the iron spin is practically constant. It might be imagined, therefore, that the longitudinal mechanism could not operate. This is true only so long as the directions of the iron spins and the RE spins are the same, as would be the case if the RE-iron interaction were isotropic. Consider, however, the case where the RE-iron coupling is anisotropic, and is of the form

$$K_1S_xJ_x+K_2S_yJ_y+K_3S_zJ_z,$$

where **S** is the total iron spin, and **J** is the "fictitious spin" describing the RE ion ground state. Here the axes (xyz) have been chosen to be the principal axes of the tensor K. The components of the iron spin, S_x, S_y, S_z, will then give rise to an exchange field with components K_1S_x, K_2S_y, and K_3S_z, so that the direction of the resultant effective exchange field (and therefore of the RE spin) will not in general be the same as the direction of the iron spin. Thus the time-varying part of the exchange field, perpendicular to the average direction of the iron spin, will then have a component parallel to the direction of the RE spin. Hence, the longitudinal mechanism can operate providing the coupling between the RE and iron spins is anisotropic. A discussion of anisotropic exchange is outside the scope of this paper, and the reader is referred to the literature.[13]

4. LONGITUDINAL RELAXATION FOR AN ISOLATED KRAMERS DOUBLET

The energy level structure of Yb^{3+} in YIG is particularly simple. The free ion is accurately described by Russell-Saunders coupling with the single term $(4f)^{13}\,{}^2F$. The large spin-orbit coupling separates the two multiplets ${}^2F_{7/2}$ and ${}^2F_{5/2}$ by 10 000 cm^{-1}, and enables them to be considered separately. The crystal

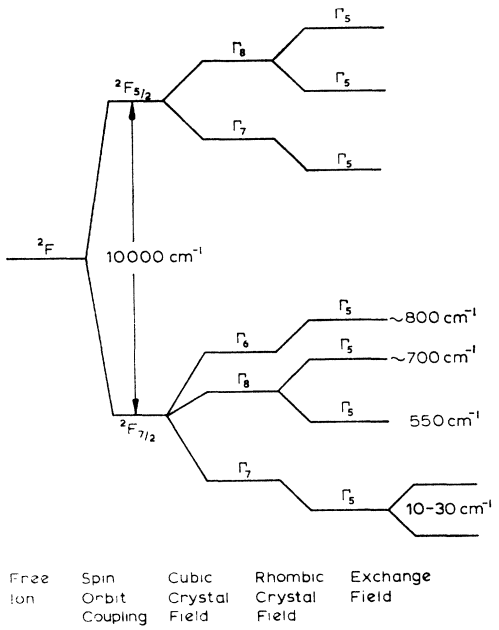

FIG. 1. The energy-level structure of Yb^{3+} in the YIG environment (diagrammatic).

field splitting of the ground multiplet covers some 800 cm^{-1} [14] and is shown diagrammatically in Fig. 1. Wickersheim and White[15] have measured the exchange interaction for Yb in Yb iron garnet (YbIG) and find it to cover the range 10–30 cm^{-1}. As this is much smaller than the separation of the ground and the first excited doublets,[14] then the exchange interaction for the ground doublet can be considered as a small perturbation on the crystal field. Admixture of higher states into the ground state will then be small, and if K is the tensor describing the exchange interaction of the ground doublet, then the Zeeman splitting of this doublet is given by

$$\hbar\omega_n=(K_1^2\bar{S}_x^2+K_2^2\bar{S}_y^2+K_3^2\bar{S}_z^2)^{1/2},$$

where the bar indicates the time-averaged components of the iron spin. This splitting is conventionally described by a tensor G, where $G=K\cdot\mathbf{S}$. We will neglect the effect on the doublet splitting of the actual field applied in the resonance experiment, since such fields are very small compared to the exchange field.

If the separation by the crystal field of the next doublet above the ground state is large compared to kT, then this and higher levels will be negligibly

[13] J. H. van Vleck, *Revista de Matemática y Física Teórica* (Tucumán, Argentina, 1962) Vol. 14, p. 189. P. M. Levy, Phys. Rev. **135**, A 155 (1964).

[14] R. Pappalardo and D. L. Wood, J. Chem. Phys. **33**, 1734 (1960); M. Ball, G. Garton, M. J. M. Leask, and W. P. Wolf, *Proceedings of the Seventh International Conference on Low Temperature Physics, 1960* (University of Toronto Press, Toronto, Canada, 1960) p. 128; Y. Ayant, J. Thomas, J. Cohen, and J. Ducloz, J. Phys. Radium **22**, 63S (1961); W. H. Brumage, C. C. Lin, and J. H. van Vleck, Phys. Rev. **132**, 608 (1963). For a review, see M. T. Hutchings and W. P. Wolf, J. Chem. Phys. **41**, 617 (1964).

[15] K. A. Wickersheim and R. L. White, Phys. Rev. Letters **8**, 483 (1962).

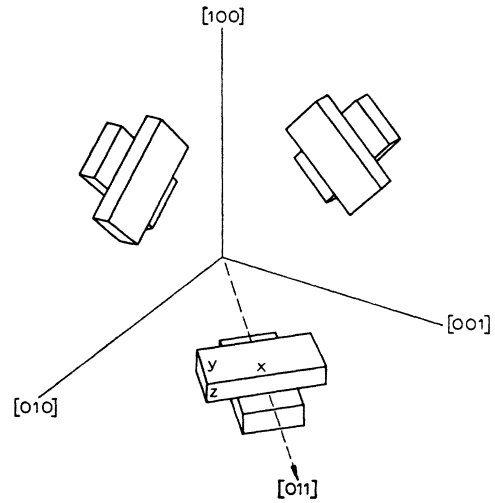

FIG. 2. Orientation of the local site axes of the RE sites relative to the crystallographic axes of the garnet unit cell [after J. F. Dillon, Jr., and L. R. Walker, Phys. Rev. **124**, 1401 (1961)].

populated, and will not therefore contribute to the required redistribution of populations. For Yb, this separation is approximately 550 cm^{-1}.[14] Thus below room temperature, Yb ions in YIG can be considered to a good approximation in the context of the longitudinal mechanism as having a single Kramers doublet.

We shall neglect cross relaxation between the Yb ions, and scattering to spin waves through the Yb ions upsetting the perfection of the YIG lattice. For the isolated Kramers doublet ground state, the following expressions are then obtained for the linewidth ΔH and the dynamic shift S_D in the field for resonance:

$$\Delta H=\frac{C}{6MkT}\sum_{n=1}^{6}A_n\frac{\omega\tau_n}{1+(\omega\tau_n)^2}\operatorname{sech}^2\left(\frac{\hbar\omega_n}{2kT}\right), \quad (1)$$

$$S_D=-\frac{C}{12MkT}\sum_{n=1}^{6}A_n\frac{(\omega\tau_n)^2}{1+(\omega\tau_n)^2}\operatorname{sech}^2\left(\frac{\hbar\omega_n}{2kT}\right), \quad (2)$$

where $\mathbf{M}=\gamma\hbar\mathbf{S}$ is the iron sublattice magnetization; C is the number of Yb ions per cc; ω is the microwave measurement frequency; $\hbar\omega_n$ is the splitting of the Kramers doublet in the direction of the iron spin, and τ_n is the Yb^{3+} ion relaxation time. The summation is over the $n=6$ different orientations of the RE site relative to the crystallographic axes, as illustrated in Fig. 2. The negative sign for S_D indicates that the dynamic shift in the field for resonance is downwards.

A_n is a function of the gradients of the doublet energy levels, and is given by

$$A_n=-\tfrac{1}{4}\{(\partial(\hbar\omega_n)/\partial\theta)^2+(\partial(\hbar\omega_n)/\partial\phi)^2\},$$

where θ and ϕ are the angular coordinates of the iron spin relative to the RE site local axes. These gradients can be related to the principal values of the tensor G. For example, for the iron magnetization directed in a (110) plane, we find[10]

$$A_n=-(2\hbar\omega_n)^{-2}\{[(G_1^2-G_2^2)(\lambda_2{}^n)^2+(G_1^2-G_3^2)(\lambda_3{}^n)^2]^2-(G_1^2-G_2^2)^2(\lambda_2{}^n)^2-(G_1^2-G_3^2)^2(\lambda_3{}^n)^2\}, \quad (3)$$

where $\lambda_i{}^n$ are the direction cosines relating the direction of the iron magnetization to the principal axes of the nth RE site. We note that with complete isotropy (i.e., $G_1=G_2=G_3$), all the A_n's are zero, and both the linewidth and the shift vanish.

For the iron magnetization in a general crystallographic direction, Eqs. (1) and (2) are complicated as A_n, $\hbar\omega_n$, and hence τ_n are different for each type of RE site. The expressions are much simplified, however, for certain symmetry directions, because of the simple relationship between the RE site axes and the crystallographic axes, as illustrated in Fig. 2. We shall explicitly evaluate the linewidth expressions for the iron magnetization directed along the principal crystallographic axes. The shift expressions can be obtained in the same way.

For the iron magnetization in the crystallographic [100] direction, four of the RE sites have equal values of A_n, which, from Eq. (3), is

$$A_n=\tfrac{1}{4}(2\hbar\omega_n)^{-2}(G_1^2-G_2^2)^2,$$

while the other two sites have $A_n=0$, and therefore do not contribute to ΔH (or the shift). The four contributing sites also have equal values of the doublet splitting:

$$(\hbar\omega_n)^2=\tfrac{1}{2}(G_1^2+G_2^2).$$

These sites will therefore also have equal values of τ_n so that for the [100] direction, Eq. (1) becomes

$$\Delta H_{100}=\frac{C}{6MkT}\left\{\frac{(G_1^2-G_2^2)^2}{2(G_1^2+G_2^2)}\right\}\left[\frac{\omega\tau_{100}}{1+(\omega\tau_{100})^2}\right]\times\operatorname{sech}^2\left(\frac{\delta_{100}}{2kT}\right), \quad (4)$$

where we have put τ_n and $\hbar\omega_n$ for the contributing sites equal to τ_{100} and δ_{100}, respectively. We note that the [100] direction magnitude depends on the difference between G_1 and G_2, and is zero if the G tensor has tetragonal symmetry. The dynamic shift in the field for resonance for the [100] direction can likewise be determined, and on division by Eq. (4) we obtain

$$\omega\tau_{100}=\frac{2|(S_D)_{100}|}{\Delta H_{100}}. \quad (5)$$

Thus, the longitudinal mechanism predicts that the relaxation time τ_{100} can be determined directly from the experimental measurements at one frequency.

A similar situation holds for the iron magnetization directed along the crystallographic [110] direction, where we again find that four sites have equal values of

A_n, while the remaining two sites have $A_n=0$. The doublet splittings of the four contributing sites are again equal, and so for the [110] direction also, the summation over the six different sites is considerably simplified, and for the linewidth we obtain

$$\Delta H_{110}=\frac{C}{6MkT}\left\{\frac{(G_1^2-G_3^2)(G_2^2-G_3^2)+\frac{3}{4}(G_1^2-G_2^2)^2}{G_1^2+G_2^2+2G_3^2}\right\}\times\left[\frac{\omega\tau_{110}}{1+(\omega\tau_{110})^2}\right]\operatorname{sech}^2\left(\frac{\delta_{110}}{2kT}\right), \quad (6)$$

where again we have set τ_n and $\hbar\omega_n$ for the contributing sites equal to τ_{110} and δ_{110}, respectively. The relaxation time for this direction can again be readily obtained from $\omega\tau_{110}=2|(S_D)_{110}|/\Delta H_{110}$.

In the [111] direction, there are two values of τ_n corresponding to the two different values of the doublet splitting, which we shall refer to as δ_1 and δ_2 where

$$(\delta_p)^2=\tfrac{1}{3}(G_3^2+2G_p^2), \quad (7)$$

where $p=1$ or 2. Each splitting corresponds to three sites with A_n values:

$$(A_n)_p=(2\delta_p)^{-2}(2/9)(G_p^2-G_3^2)^2.$$

Hence the summation over the six sites is still quite complicated for the [111] direction, and the linewidth expression is

$$\Delta H_{111}=\frac{C}{6MkT}\sum_{p=1}^{2}\left\{\frac{(G_p^2-G_3^2)^2}{2(2G_p^2+G_3^2)}\right\}\left[\frac{\omega\tau_p}{1+(\omega\tau_p)^2}\right]\times\operatorname{sech}^2\left(\frac{\delta_p}{2kT}\right). \quad (8)$$

A relaxation time for this direction can still be defined by the equation

$$\omega\tau_{111}=\frac{2|(S_D)_{111}|}{\Delta H_{111}}. \quad (9)$$

This will be a weighted average of the two actual relaxation times, τ_1 and τ_2, in this direction. The weighting will depend on temperature as well as on the G tensor, but can be determined from Eq. (8) and the corresponding expression for the dynamic shift through the definition of τ_{111}, Eq. (9).

It is convenient here to examine the temperature dependences predicted for the linewidth and the dynamic shift in the principal crystallographic directions. The term in $(1/kT)\operatorname{sech}^2(\delta/2kT)$ common to both ΔH and S_D arises from the difference in populations between the contributing doublet levels, and is a maximum when T (in °K) equals $0.93\times\delta$ (in cm^{-1}). The position in temperature of this maximum is independent of the measurement frequency, ω. The terms in $\omega\tau$ will also be temperature-dependent, as τ will decrease with increasing temperature. The $\omega\tau$ term in the linewidth expression will be a maximum at the temperature where $\omega\tau=1$. The temperature of this maximum will thus depend on the measurement frequency according to the temperature dependence of τ. The $\omega\tau$ term in the shift expression will be unity for $\omega\tau\gg1$, zero for $\omega\tau\ll1$ and will pass through the value $\frac{1}{2}$ at $\omega\tau=1$. Thus, as a function of temperature, the dynamic shift shows a single maximum whilst the linewidth can show two maxima. We cannot say *a priori* which of the terms in the linewidth will peak at the lower temperature, but a comparison with the shift maximum, or measurement at more than one microwave frequency, will indicate the order. It may be, of course, that only a single peak is seen in the $\Delta H(T)$ plot if the particular values of δ and ω, and the magnitude and temperature dependence of τ, are such that the two maxima are not resolved.

At low temperatures, the predicted temperature dependence of ΔH (and S_D) becomes very strong as the ability of the RE ions to relax the precession of the iron sublattice is reduced through depopulation of the upper level of the ground doublet. For $kT<\delta/2$, the sech^2 term becomes an exponential, and we find a temperature dependence:

$$\Delta H\propto(1/T)(\omega\tau/[1+(\omega\tau)^2])\exp(-\delta/kT). \quad (10)$$

We shall find below that the term in $\omega\tau$ is slowly varying with temperature at these low temperatures compared to the exponential term, so that further information on δ (and hence on the G tensor) can be obtained directly from a plot of $\log(T\Delta H)$ versus $1/T$ for this low-temperature region.

5. EXPERIMENTAL RESULTS

Measurements of field for resonance and linewidth were made near 9.3 Gc/sec and 16.8 Gc/sec over the temperature range 1.5–300°K on a single crystal specimen of Yb-doped YIG for which chemical analysis gave the composition $(Yb_{0.051}Y_{0.949})_3Fe_5O_{12}$. The crystal was grown from the melt, using a PbO/PbF_2 flux. A spherical specimen (0.42-mm diam, with a variation in diameter less than ±4 parts in 10 000) was prepared using in turn a Bond-type air blower[16] and a two-tube method.[17] This latter device was used with one-micron-grade diamond polishing paste, though the method leaves a few scratches of a slightly larger size.

In Fig. 3 we show the variation of linewidth with temperature for the [111] and [100] directions at the two measurement frequencies. The dynamic shifts for these directions at the same frequencies are shown in Fig. 4. In the [110] direction, the resonance line is broadened and shifted anomalously at low temperatures,[18] and we shall only make little use in this paper of measurements in this direction.

[16] W. L. Bond, Rev. Sci. Instr. **22**, 344 (1951).
[17] P. H. Cross, Rev. Sci. Instr. **32**, 1179 (1961).
[18] J. F. Dillon, Jr., J. Appl. Phys. **32**, 159S (1961).

The shifts have been obtained by using the relation

$$H_r=(\omega/\gamma)+H_a-H_{se}+S_D,$$

where H_r is the measured field for resonance and H_a is the anisotropy field in the absence of relaxation effects. H_{se} is a small correction, determined empirically, allowing for the sample size.[19] We obtain H_a from measurements by the torque method,[20] for which ω is essentially zero, since the direction of the exchange field is here changed very slowly, allowing ample time for the required redistribution of populations. Owing to the dependence of the shift S_D on frequency, values for γ cannot be obtained experimentally in the usual way from the difference in the resonance fields at two frequencies, excepting at temperatures where $\omega\tau\gg1$ or $\omega\tau\ll1$. We have therefore calculated γ from the relation[21]

$$\gamma=\left(\frac{e}{2mc}\right)\frac{M_{\mathrm{Fe}}+x\sum_n m_n}{(M_{\mathrm{Fe}}/g_{\mathrm{Fe}})+x\sum_n (m_n/g_{\mathrm{Yb}})},$$

where m_n is the moment per Yb ion, x is the level of doping (here equal to 0.051) and the summation is over the six inequivalent sites. In calculating m_n and the Yb g factor, g_{Yb}, we have made use of the value of the G tensor measured in YbIG [15] and of measurements of the paramagnetic G tensor of Yb gallium garnet (YbGaG).[22] For g_{Fe}, we have taken the value 2.01 as indicated by our measurements on undoped YIG. The values of γ so calculated are in good agreement with the experimental values below 10°K where we shall find $\omega\tau\gg1$, and above 250°K, where we shall find $\omega\tau\ll1$.

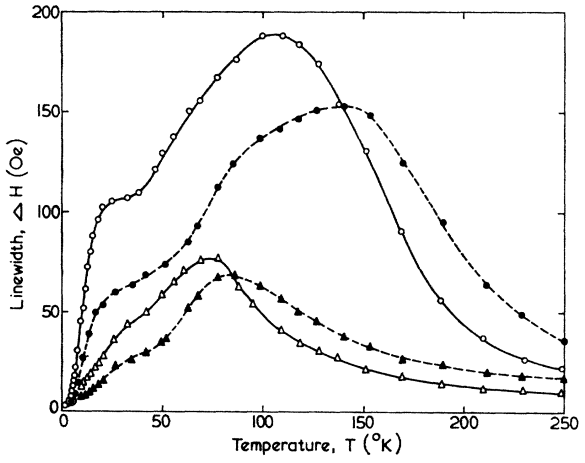

FIG. 3. Linewidth versus temperature for 5.1% Yb in YIG in the [111] direction (circles) and the [100] direction (triangles) at 9.3 Gc/sec (open symbols) and 16.8 Gc/sec (closed symbols).

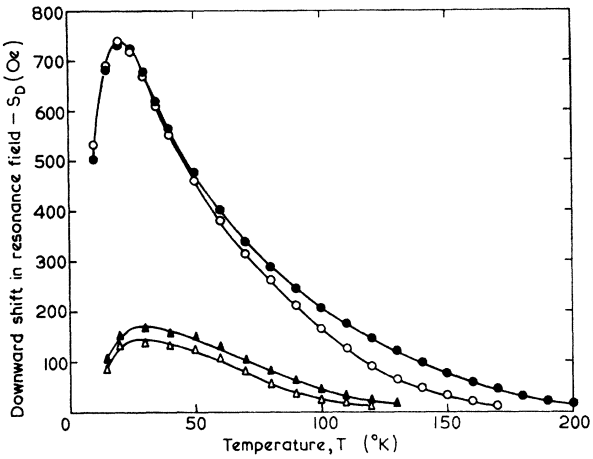

FIG. 4. Dynamic shift in the field for resonance (see text) versus temperature for 5.1% Yb in YIG. Legend as Fig. 3.

A qualitative examination of Figs. 3 and 4 shows that the temperature dependences exhibit the main features discussed at the end of Sec. 4. We shall now make a quantitative comparison between the experimental results and those predicted by the longitudinal mechanism, and deduce the G tensor and relaxation times which best fit the relevant equations in Sec. 4.

6. THE G TENSOR

We can determine the average value of the doublet splitting in the [111] direction, δ_{111}, from the plot of $\log(T\Delta H_{111})$ versus $1/T$ at low temperatures (see Eq. 10). The details have already been published.[23] The result is 21.0 cm^{-1}. This is a weighted average of the two actual splittings, δ_1 and δ_2, as given by Eq. (7). We must determine the weighting in order to deduce either δ_1 or δ_2. Calling the associated relaxation times τ_1 and τ_2, respectively, we have for $kT<\delta/2$

$$T\Delta H_{111}\propto\sum_{p=1}^{2}(A_p/\tau_p)\exp(-\delta_p/kT).$$

Here we have used $\omega\tau_p\gg1$, as indicated by the relaxation time results presented in the next section. These results also show that $(1/\tau_p)=(1/\tau_p{}^0)\coth(\delta_p/2kT)$ at these low temperatures (see Sec. 8) so from Eq. (8) we obtain

$$T\Delta H_{111}\propto\exp\left(-\frac{\delta_1}{kT}\right)\left[1+\frac{(G_2{}^2-G_3{}^2)^2}{(G_1{}^2-G_3{}^2)^2}\frac{(2G_1{}^2+G_3{}^2)}{(2G_2{}^2+G_3{}^2)}\times\left(\frac{\tau_1{}^0}{\tau_2{}^0}\right)\exp\left(\frac{\delta_1-\delta_2}{kT}\right)\right]. \quad (11)$$

[19] B. H. Clarke, Mullard Research Laboratories, No. 478, 1963 (unpublished).
[20] R. F. Pearson, Proc. Phys. Soc. (London) **74**, 505 (1959).
[21] N. Tsuya, Progr. Theoret. Phys. (Kyoto) **7**, 263 (1952); R. K. Wangsness, Phys. Rev. **91**, 1085 (1953).
[22] D. Boakes, G. Garton, D. Ryan, and W. P. Wolf, Proc. Phys. Soc. (London) **74**, 663 (1959); J. W. Carson and R. L. White, J. Appl. Phys. **31**, 53S (1960).
[23] B. H. Clarke, J. Appl. Phys. **36**, 1211 (1965).

Thus the splitting δ_1 can be obtained from the low-temperature [111] linewidth provided we can evaluate the weighting term contained in square brackets in Eq. 11.

In principle, the active splitting in the [100] direction, δ_{100}, can similarly be determined from the plot of $\log(T\Delta H_{100})$ versus $1/T$ at low temperatures. In practice, we run into difficulties, for we find a residual linewidth of ~8–10 Oe at the lowest temperatures. This is a rather larger value than is to be expected from the host YIG.[23] The explanation is probably trivial to the extent that it is a measurement effect associated with [100] being a hard direction of magnetization. Any misalignment of the applied field direction relative to the [100] direction produces an even bigger deviation in the magnetization direction (according to the relative sizes of the applied and anisotropy fields) with a consequent error in the measured parameters. With the misalignment of the field direction found in practice ($<1°$) the error is negligible excepting at temperatures below about 20°K, where the anisotropy field increases rapidly with lowering temperature. Even here the effect is small as indicated by the residual linewidth given above, but is sufficient to prevent quantitative interpretation of the low temperature results for the [100] direction. However, we can deduce δ_{100} approximately from the temperature of the maximum shift, which indicates a value in the region of 25–30 cm^{-1}.

More information on the G tensor can be obtained from the linewidth at higher temperatures. For $kT>\delta$, the sech^2 term is not sensitive to the particular choice of δ and the magnitudes of the terms $\sum_n A_n$ for the [100] and [111] directions can be determined from Eqs. (4) and (6), using values of the relaxation time as presented in Sec. 7. For the [111] direction, we assume that the relaxation times corresponding to the two values of the doublet splitting are equal at these higher temperatures where the Raman relaxation process dominates. After converting the magnitudes to 0°K by assuming that the doublet splitting varies with temperature in the same way as the iron sublattice magnetization, we obtain the following values:

[100] direction:

$$\frac{(G_1^2-G_2^2)^2}{2(G_1^2+G_2^2)}=85\ (\mathrm{cm}^{-1})^2;$$

[111] direction:

$$\frac{1}{2}\left\{\frac{(G_1^2-G_3^2)^2}{2G_1^2+G_3^2}+\frac{(G_2^2-G_3^2)^2}{2G_2^2+G_3^2}\right\}=308\ (\mathrm{cm}^{-1})^2.$$

These equations, together with the relation

$$(\delta_1)^2=\tfrac{1}{3}(G_3^2+2G_1^2),$$

can be solved to give G_1, G_2, and G_3. For a first estimate of δ_1, we have used Wickersheim and White's result for the G tensor of Yb in YbIG [15] to determine the weighting term in Eq. (11). The G tensor solution obtained can then be used to re-estimate the weighting term. Obviously, the whole process can be iterated until a stationary solution is obtained.

We note that the weighting term depends not only on the G tensor, but also on the ratio (τ_1^0/τ_2^0). We shall again anticipate the relaxation-time results, which indicate that the spin-magnon relaxation is the dominant relaxation process for the [111] direction in the low-temperature region. The value of τ_p^0 for the spin-magnon process has been related to the G tensor by Huber.[24] The relations can be included in the above iterative procedure, and the final G tensor obtained is then

$$G_1=31.9\ \mathrm{cm}^{-1},$$
$$G_2=22.4\ \mathrm{cm}^{-1},$$
$$G_3=\ 8.5\ \mathrm{cm}^{-1}.$$

The values determined spectroscopically by Wickersheim and White for Yb in YbIG [15] are: $G_1=30.6\ cm^{-1}$; $G_2=26.1\ cm^{-1}$; and $G_3=11.8\ cm^{-1}$, which are similar to our values. This is quantitative evidence of the ability of the longitudinal mechanism to explain the observed linewidths. Nevertheless, there are significant differences in detail. Such differences are to be expected because the bigger lattice dimensions of YIG compared with YbIG will undoubtedly affect the size of the exchange interactions. Indeed, Wickersheim[25] has reported that his optical measurements indicate that the over-all splitting is smaller for 1% Yb in YIG than in YbIG by about 7%. In fact, we find that the difference is not isotropic, which is not surprising since the exchange interaction itself is anisotropic.

Further evidence of a real difference between the G tensors of the 5% and 100% dopings is indicated by calculation of the static torque curves, for which our G tensor gives closer agreement than Wickersheim and White's with the experimental torque curves measured at 4.2°K on a sample of 5.1% Yb in YIG taken from the same crystal as the sample used in the present work.[26]

In deriving the G tensor, it will be noted that we have not made use of any measurements in the [110] direction. This is because in this direction the linewidth is anomalously broadened at low temperatures,[18,27] as we have already mentioned. Thus below about 20°K, the linewidth is proportional to $1/T$, and also proportional to ω. This behavior is indicative of the excitation of direct transitions across a near crossover in the ground-doublet energy levels.[28] However, the G tensor

[24] D. L. Huber, Phys. Rev. **136**, A500 (1964).
[25] K. A. Wickersheim, Phys. Rev. **122**, 1376 (1961).
[26] R. F. Pearson (to be published).
[27] B. H. Clarke (to be published).
[28] C. Kittel, Phys. Rev. Letters **3**, 169 (1959); C. Kittel, Phys. Rev. **117**, 681 (1960).

that we have deduced above does not describe such a near crossover, and therefore we cannot account for the presence of the anomalous line broadening in this direction. At temperatures above about 20°K, the [110] linewidth varies with temperature and frequency as expected on the basis of the longitudinal mechanism. If we subtract out the extrapolated anomaly contribution, the linewidths yield a value of 283 $(cm^{-1})^2$ for the term $\sum_n A_n$, corrected to 0°K, in the [110] direction. By comparison, the G tensor we have deduced above implies a value of 362 $(cm^{-1})^2$, from the term in curly brackets in Eq. (6). Thus apart from the low temperature anomaly, the linewidths in the [110] direction are roughly consistent, on the basis of the longitudinal mechanism, with those in the other principal directions.

In principle, the G tensor can also be derived from the dynamic shifts, S_D, but as they are more difficult to determine and less accurate than the linewidths, we have not attempted such an analysis. However, the observed dynamic shifts are in good agreement with the above G tensor and the relaxation times as presented in Sec. 7.

7. RELAXATION TIMES: EXPERIMENTAL RESULTS

Figure 5 shows the inverse of the relaxation times for the [111] and [100] directions as a function of temperature. For the [100] direction, and for the [111] direction up to 160°K, the results have been determined from the relation $2|S_D|/\Delta H$ [Eqs. (5) and (9)]. The agreement, within likely experimental error, between the results determined at the two different measurement frequencies is further quantitative evidence of the ability of the longitudinal mechanism in explaining the relaxation properties. The [100] direction results are less accurate, and more limited, than the [111] direction results because the shifts are smaller and therefore more difficult to determine in the former direction. For the same reason, the values at the ends of the temperature ranges will be less accurate than the values in the middle, for both directions. The shifts in the [111] direction become too small to measure accurately at temperatures above 160°K although the linewidths are still appreciable. We have therefore determined τ for this direction for the temperature range 160–240°K from the linewidth alone. Now at these higher temperatures, τ is becoming increasingly short, and we must bear in mind the possibility of some linewidth contribution from the transverse mechanism[5] as $\omega_n\tau$ approaches unity. We have therefore equated the experimental linewidth to the sum of the predicted linewidths from both longitudinal and transverse mechanisms. We have used the G-tensor values deduced above to determine the other terms in these equations, and have solved for τ. In fact, the transverse mechanism linewidth contributions turn out to be negligible below 250°K, and essentially the same values of the relaxation time are obtained by ascribing the observed linewidths to the longitudinal mechanism only.

We have also deduced some relaxation times for the [110] direction in the high-temperature region, 100–240°K, from the linewidth only, after subtracting out the extrapolated anomaly contribution. We have evaluated $(T\Delta H)/\mathrm{sech}^2(\delta/2kT)$ [see Eq. (6)] as a function of T, and have normalized the maximum value to $\frac{1}{2}$, and have solved for τ. Within experimental error, these relaxation times are the same as those found for the [111] direction.

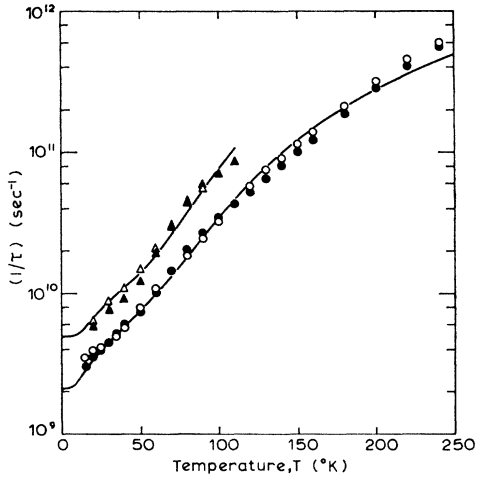

FIG. 5. Inverse relaxation times versus temperature for 5.1% Yb in YIG, legend as Fig. 3. The lines are plots of the function $(1/\tau^0)_D \coth(\delta/2kT)+AJ_8T^9$ (see text) with $(1/\tau^0)_D=2.1\times10^9$ sec^{-1}, $\delta=21.0$ cm^{-1}, and $A=4.5\times10^{-12}$ sec^{-1} $(°K)^{-9}$ for the [111] direction, and with $(1/\tau^0)_D=5\times10^9$ sec^{-1}, $\delta=27.5$ cm^{-1}, and $A=1.4\times10^{-11}$ sec^{-1} $(°K)^{-9}$ for the [100] direction.

8. RELAXATION TIMES: DISCUSSION

We will now compare the relaxation time results with theories of the relaxation time of the Yb ion in the YIG environment.

Theories of the spin-lattice relaxation time can be conveniently divided into two groups, first-order (or single-phonon) and second-order (or two-phonon) processes, according to the number of phonons involved in the relaxation. In the second-order process, the ion is relaxed across the ground state through a higher state by the annihilation and creation of phonons whose energies differ by that of the ground-doublet splitting. This is known as the resonance or Orbach process,[29,30] where the higher state is a real crystal-field level, and the Raman process when virtual levels are involved. As both these processes require the presence of phonons of high energy compared to the ground-doublet splitting,

[29] R. Orbach, Proc. Roy. Soc. (London) **A264**, 458 (1961).

[30] R. Orbach, J. Appl. Phys. **33**, 2144 (1962); also, in *Proceedings of the First International Conference on Paramagnetic Resonance* (Academic Press Inc., New York, 1963), p. 456.

they are dominated at low temperatures by the first-order or direct process. Here the ion is relaxed by the creation or annihilation of a single phonon of energy equal to that of the doublet splitting. This process has been extensively studied by Orbach.[29,30] All these processes also occur in paramagnetic relaxation (where a real field is applied to raise the Kramers degeneracy) and below we shall make use of results on Yb in YbGaG.

In the above processes, the RE spin is coupled to the lattice through the spin-orbit interaction and the modulation of the crystal field by the phonons. In a ferrimagnetic material, we also have the possibility of spin-lattice coupling through modulation of the exchange field either by phonons or by magnons. For the latter, Huber[24] has calculated the relaxation time for the direct process, and we shall show below that this spin-magnon process better describes the observed direct process than does the spin-lattice process. Spin-magnon relaxation is not likely to be important with regard to the second-order processes in view of the higher energies involved, and will not be considered further. We shall show below that spin-lattice relaxation adequately describes the observed second-order processes.

A. The Direct Process

The direct process spin-lattice relaxation time has been calculated by Orbach,[29,30] and can be written in the form

$$1/(\tau_{sl})_D=(1/(\tau_{sl}{}^0)_D)\coth(\delta/2kT), \qquad (12)$$

where $(1/\tau_{sl}{}^0)_D$ is the relaxation time at $T=0°$K. Since both phonons and magnons are bosons, the spin-magnon relaxation time has the same temperature dependence, though, of course, the spin-magnon coefficient $(1/\tau_{sm}{}^0)_D$ contains different terms to the spin-lattice coefficient $(1/\tau_{sl}{}^0)_D$.

Our results indicate that in the [111] direction, the above temperature dependence is followed up to a temperature of $\sim 60°$K. The best fit gives a value of the coefficient, $(1/\tau_{111}{}^0)_D$, of 2.1×10^9 sec^{-1}. We must remember that our experimental relaxation time in this direction is a weighted average of the two actual relaxation times, but since $\omega\tau\gg 1$ at these temperatures, the weighting simply depends on the relative sizes of $(A_n)_p\,\mathrm{sech}^2(\delta_p/2kT)$ for the two values of the doublet splitting, and can therefore be determined from the G tensor.

Huber's paper[24] contains the calculation of the spin-magnon coefficients, and the reader is referred to this paper for the full formula. We have used Huber's formula to calculate the spin-magnon coefficients for the G tensor we have deduced above, using the same values as Huber for the other terms. We obtain the values 8.8×10^8 sec^{-1} and 2.40×10^9 sec^{-1} corresponding to the two splittings, δ_1 and δ_2, respectively. To compare with the experimental coefficient, we have weighted these coefficients as indicated above, using $T\simeq 30°$K, since it is from fitting the experimental results in this region of temperature that we have deduced our experimental coefficient. The averaged spin-magnon coefficient is then 2.15×10^9 sec^{-1}, in excellent agreement with the observed value.

We recall that the G tensor used to calculate $(1/\tau_{sm}{}^0)_D$ was itself derived iteratively by using the ratio $(\tau_1{}^0/\tau_2{}^0)$ as indicated by the spin-magnon coefficients. Thus the spin-magnon direct process gives a consistent solution both for the G tensor and the [111] direction average direct process relaxation time.

But what of the spin-lattice direct process? Svare and Seidel[31] have measured the relaxation time for Yb in YbGaG, which has closely similar crystal field parameters to YIG,[14] and probably a similar phonon spectrum. They find a direct process dominant at low temperatures, with a value of the coefficient of 6.88 sec^{-1} for a field induced splitting of the Kramers doublet of 0.29 cm^{-1}. Orbach[29,30] has calculated that the spin-lattice coefficient is proportional to δ^3 and to the square of the matrix element coupling the spins and the phonons. In the crude approximation that the orbit-lattice interaction is independent of the exchange interaction, this matrix element is just proportional to the splitting of the Kramers doublet, so that $(1/\tau_{sl}{}^0)_D \propto \delta^5$. Svare and Seidel's result then extrapolates to give coefficients of 4.4×10^{10} sec^{-1} and 8.1×10^9 sec^{-1} for our values of δ_1 and δ_2, respectively. Although these values are too short to explain the observed direct process for the [111] direction, we cannot place too much importance on the exact magnitudes in view of the approximation made in, and the wide range covered by, the extrapolation. The importance of the extrapolation is that it indicates that spin-lattice relaxation might be of importance in considering the observed direct process. However, if, in the iterative procedure to determine the G tensor, we use the ratio $(\tau_1{}^0/\tau_2{}^0)$ as indicated by the spin-lattice coefficients, we obtain a negative value for $G_3{}^2$. Comparing this with the consistent agreement obtained using the spin-magnon coefficients, we conclude that the spin-lattice relaxation does not make a significant contribution to the observed direct process relaxation time, in which case the spin-lattice coefficients must be not greater than about 10^8 sec^{-1}. This would indicate a disagreement of some two orders of magnitude between the spin-lattice direct process relaxation times of Yb in YIG and in YGaG, on the basis that $(1/\tau_{sl}{}^0)_D$ is proportional to δ^5. It is interesting to note that Orbach[30] has estimated the terms in the coefficients $(1/\tau_{sl}{}^0)_D$ for the case of Yb in YIG, and obtains $\sim 10^7$ sec^{-1}.

Let us now examine the relaxation time results in the [100] direction. Though less precise than those in

[31] I. Svare and G. Seidel, *Proceedings of the First International Conference on Paramagnetic Resonance* (Academic Press Inc., New York, 1963), p. 430.

the [111] direction, they nevertheless suggest the predominance of a direct process for $T<60°K$. The best fit to Eq. (12) gives a coefficient value of the order of 4×10^9 sec^{-1}. The spin-magnon calculation for this direction yields a coefficient value of 1.8×10^9 sec^{-1}. The agreement between the spin-magnon and experimental values is therefore not so exact in this direction as it was in the [111] direction. Though the likely experimental inaccuracy in the [100] direction relaxation times prevents us placing too much emphasis on the discrepancy, it is possible that it indicates a significant spin-lattice contribution in this direction. It is in the [100] direction that the spin-lattice relaxation time is expected to be shortest, since this is the direction with the widest splitting, although the contribution required ($\sim2\times10^9$ sec^{-1}) is rather bigger than expected in view of the conclusions reached for the [111] direction.

B. Second-Order Processes

For $T>70°K$, the second-order processes dominate, and the experimental relaxation times are shorter than those predicted by the direct process. In Fig. 6 we have plotted, against $1/T$, the [111] direction inverse relaxation times remaining after subtracting out the average direct process contribution, $2.1\times10^9\times\coth(15.1/T)$ sec^{-1}.

The relaxation time due to the Raman process[29] can be written in the form

$$(1/\tau)_R=AJ_8T^9,$$

where $J_8=\int_0^x\{(x^8e^x)/(e^x-1)^2\}dx$ with $x=\Theta_D/T$ where Θ_D is the Debye temperature, which for YIG is of the order of 550°K.[32] The relaxation time due to the Orbach process is given by [29,30]

$$(1/\tau)_O=(B/[\exp(\Delta/kT)-1]),$$

where Δ is the crystal field splitting between the ground and first excited doublets, and is ~550 cm^{-1}.

Orbach has calculated the terms in the coefficients A and B in the general case.[29] He has also estimated the magnitudes of the quantities involved for the case of Yb in YIG,[30] and finds that the Raman term should be unimportant, and that the dominant second-order mechanism should be the Orbach process with a coefficient of the order of 10^{11} sec^{-1}. We have tried fitting the Orbach term alone to the experimental second-order relaxation times. Using the above value of Δ, the best fit is obtained with $B=2.6\times10^{13}$ sec^{-1}, but as will be seen from Fig. 6, the fit is not very good. A more acceptable fit can be obtained using a value for Δ of 346 cm^{-1}, with $B=6.2\times10^{10}$ sec^{-1}. Although Wood[33]

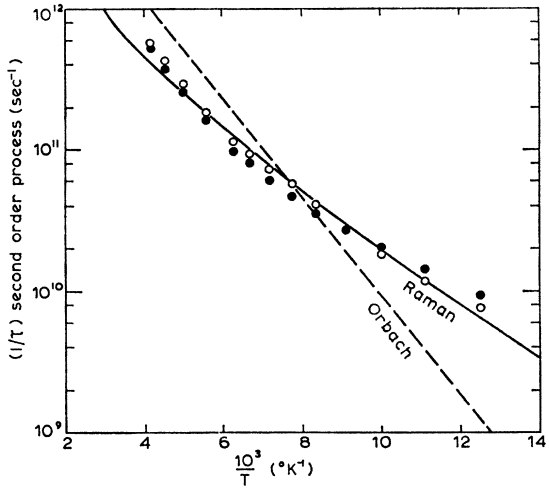

FIG. 6. Second order process inverse relaxation times for the [111] direction (see text) versus $1/T$ for 5.1% Yb in YIG. The solid line is a plot of the Raman term AJ_8T^9 with $A=4.5\times10^{-12}$ sec^{-1} (°K)$^{-9}$ and using $\Theta_D=550$°K. The dashed line is a plot of the Orbach term $B/[\exp(\Delta/kT)-1]$ with $\Delta=550$ cm^{-1} and $B=2.6\times10^{13}$ sec^{-1}.

has suggested the presence of a crystal field level at 308 cm^{-1} above the ground state from measurements of the optical absorption spectrum of Yb doped YGaG, other evidence[14] suggests that this spectral line should be identified with lattice vibrations, and that the crystal field separation of the first excited doublet is 550 cm^{-1}. We conclude that the Orbach term cannot account for the experimental results.

If we fit the sum $(1/\tau)_R+(1/\tau)_O$ to the experimental second-order process relaxation times using $\Theta_D=550$°K and $\Delta=550$ cm^{-1}, we find the best fit with $A=4.5\times10^{-12}$ sec^{-1}(°K)$^{-9}$ and with B not greater than about 2×10^{12} sec^{-1}. That is to say, the experimental second-order relaxation times are best described by the Raman term alone, and that the relaxation time from the Orbach process is too long to make a significant contribution anywhere in the temperature range covered here. The fit obtained using the Raman term alone with the above value of A is also shown in Fig. 6.

Though our value of A is some 5 orders of magnitude bigger than the theoretical estimate,[31] it is in good agreement with the measurements of Svare and Seidel[31] for Yb in YbGaG, for which they observed a Raman process with $AJ_8=1.8\times10^{-7}$ sec^{-1}(°K)$^{-9}$ in the temperature range 10–20°K, which is equivalent to a value of A of 4.5×10^{-12} sec^{-1}(°K)$^{-9}$. It thus seems that the Raman process relaxes the Yb ion in the garnet lattice much more rapidly than expected, though we can offer no explanation why this is so.

The Raman process with this same coefficient would also fit the relaxation times we have been able to deduce for the [110] direction between 100–240°K, if the direct process contributions were much the same as in the [111] direction. In the [100] direction, the relaxa-

[32] A. B. Harris and H. Meyer, Phys. Rev. **127**, 101 (1962); D. Edmonds and R. Petersen, Phys. Rev. Letters **2**, 499 (1959); J. E. Kunzler, L. R. Walker, and J. R. Galt, Phys. Rev. **119**, 1609 (1960); S. S. Shinozaki, *ibid.* **122**, 388 (1961).

[33] D. L. Wood, J. Chem. Phys. **39**, 1671 (1963).

tion times, after making due allowance for the direct-process contribution, are also in agreement with the Raman term but with a value of A some 2.5 times larger than that found for the [111] direction.

Because of the dominance of the Raman process, we cannot say from our data whether or not Orbach's estimate of B is in accordance with experiment. We would like to point out, however, that for Yb in YIG, Δ is greater than $k\Theta_D$, so that if the phonon spectrum were of the simple Debye form, the Orbach process would not be able to occur at all since phonons of energy Δ would not be available. In fact the YIG phonon spectrum will certainly be more complex than the simple Debye form, and the high-energy tail may reach as high as Δ. Thus the Orbach process may be present, but will be a much less efficient relaxation mechanism than would be the case if Δ were less than $k\Theta_D$. This point seems to have been overlooked in previous estimates of the coefficient B.

9. CONCLUSIONS

We have examined the linewidth and the dynamic shift in the field for resonance predicted, under certain assumptions, by the longitudinal (so-called "slow relaxing ion") mechanism of relaxation, and have made quantitative comparisons with microwave resonance measurements in the principal crystallographic directions of a single crystal specimen of YIG doped with 5.1% Yb. Except for an anomalous line broadening and shifting in the [110] direction at temperatures below about 20°K, these measurements are in excellent agreement with the predicted form.

We have deduced the tensor G describing the anisotropic exchange splitting of the ground state Kramers doublet of the Yb^{3+} ion, and find: $G_1=31.9$ cm^{-1}; $G_2=22.4$ cm^{-1}; $G_3=8.5$ cm^{-1}. These results are similar to those reported by Wickersheim and White from spectroscopic measurements on YbIG, and we have suggested that the difference probably reflects the different lattice dimensions in the two cases.

We have also deduced the relaxation time of the Yb^{3+} ion in the YIG environment, and have obtained the most extensive and accurate results in the [111] direction. Here we have found that the temperature dependence for $T<60$°K indicates the dominance of a direct process. Having made allowance, as indicated by the G tensor, for the fact that the measured relaxation time in this direction is a weighted average of the two actual relaxation times associated with the two values of the doublet splitting, we have found that the observed direct process is well described by spin-magnon relaxation, which also allows a more consistent evaluation of the G tensor than does spin-lattice relaxation. Our analysis suggests that extrapolation [on the basis that $(1/\tau_{sl}^0)_D \propto \delta^5$] of the spin-lattice direct process relaxation times reported by Svare and Seidel for Yb in YGaG gives results shorter than expected by at least two orders of magnitude, and that Orbach's estimate of $(1/\tau_{sl}^0)_D$ for Yb in YIG may be quite reasonable.

At higher temperatures, we have found that the temperature dependence of the relaxation time deduced in the [111] direction is best described by the Raman process, and is in excellent agreement with the Raman process relaxation time reported by Svare and Seidel for Yb in YGaG, though it is some five orders of magnitude shorter than expected theoretically. We have found the Orbach process to be unimportant in the temperature region covered by this work, and have suggested that this is to be expected.

The fit to the experimental relaxation times in the [111] direction of the combined direct and Raman processes as given by

$$\frac{1}{\tau}=\{(2.1\times10^{9})\coth(15.1/T)+(4.5\times10^{-12})J_8T^9\}\ \text{sec}^{-1}$$

is shown in Fig. 5.

The relaxation times we have deduced in the [100] direction are more limited than those obtained in the [111] direction, but suggest that here too a direct process dominates for $T<60$°K and that a Raman process dominates at higher temperatures.

ACKNOWLEDGMENTS

The authors would like to thank Dr. R. F. Pearson for supplying static-torque measurements, and J. L. Page for his careful preparation of the single-crystal specimen.